

# DETOUR trials: the mission and its results

Vojtech Stejskal\*, Heiner Kuschel\*\*,  
Tadeusz Brenner\*\*\*, Leszek Lamentowski \*\*\*, Idar Norheim-Næss\*\*\*\*,  
Piotr Samczynski\*\*\*\*\*, Janusz Kulpa\*\*\*\*\*,

\* ERA a.s.  
Prumyslova 387, 530 02 Pardubice, CZECH REPUBLIC  
email: v.stejskal@era.aero

\*\* Fraunhofer Institute for High Frequency Physics and Radar Techniques (FHR)  
Fraunhoferstraße 20, 53343 Wachtberg, GERMANY  
email: heiner.kuschel@fhr.fraunhofer.de

\*\*\* PIT-RADWAR S.A.  
Poligonowa 30, Warszawa, POLAND  
email: tadeusz.brenner@pitradwar.com

\*\*\*\* Norwegian Defence Research Establishment (FFI)  
P.O. Box 20, 2027 Kjeller, NORWAY  
email: idar.norheim-nass@ffi.no

\*\*\*\*\* Warsaw University of Technology, Institute of Electronic Systems  
Nowowiejska 15/19, 00-665 Warsaw, POLAND  
email: psamczyn@elka.pw.edu.pl

**Abstract:** In this paper DMPAR Evaluation Trials for Operationally Upgraded Radar (DETOUR) and their results for a selected scenario are described. The DETOUR trials were conducted by the SET-195 research task group (RTG) under an umbrella of NATO Science and Technology Organization from September 1 to 4, 2014 as a part of the DMPAR (Deployable Multi-band Passive/Active Radar) algorithms' evaluation process. An idea of DMPAR was to combine active and passive surveillance components in a collocated and distributed net of sensors, which would bring multiple benefits. By focusing on one of the trial scenarios, the paper describes all of them, in a form of the measured data analysis. Beside the trials, positive aspects of the combined active and passive surveillance components are discussed.

## 1. Introduction

In early 2013 NATO RTG SET-152 proposed a short-term solution as an outcome of the multi-national NATO SET RTG study on the potentials of Deployable Multi-band Passive/Active Radar (DMPAR) for air surveillance and air defense [1]. The intent of this short-term solution was to benefit from the expected performance improvements without waiting for a full development of the new sensor. Following this proposal, SET-195 RTG was formed to prove experimentally the desirable improvements in the combined processing of state-of-the-art passive radar sensors and active multi-band radar sensors in a multi-national, multi-sensor, and multi-band measurement campaign set with the following objectives:

- verification of mutual beneficial properties of multiple radar bands,
- verification of mutual beneficial properties of passive and active radar modes,

- quantification of DMPAR short-term solution benefits by means of the chosen measurements.

The DMPAR Evaluation Trials for Operationally Upgraded Radar (DETOUR) took place in the Hradec Kralove district in the Czech Republic in 2014 with the use of passive experimental radars and radar demonstrators from research institutes and universities, an industrial passive radar prototype from the host nation, and a dual-band active radar prototype [2].

Several relevant military scenarios were defined characterized by trajectories with current stand-alone active radars having target detection and tracking insufficiencies. During this one-week trial multiple sorties with different military and civilian targets were performed, providing terabytes of recorded raw radar data for further off-line individual processing in accordance with the DMPAR processing scheme.

During the first phase target detection performance was evaluated independently for each sensor by its provider. Then, in the following phase a scenario prioritization based on respective sensor data availability approach and target performance capability over the whole sensor set was applied as an input to MIMO (Multiple Input Multiple Output) based DMPAR-processing.

## 2. Scenarios and the targets

The Hradec Kralove district in the Czech Republic is dominated by a relatively flat area in the south with the hills in the north and the mountains in the northeast. Sensors for trial purposes and scenario objective reasons were deployed in three different locations: the Hradec Kralove Airport (a trial home-base), a Jaromer airfield and a Chotec airfield. Each of the selected places has the characteristics which correspond to features of a concept of collocated monostatic/multistatic passive/active radars.

The reason for selecting these areas was also ground truth data availability in a form of the Wide Area Multilateration (WAM) system, which to all sensor locations provided real-time surveillance information about targets of interest [3][2][4].

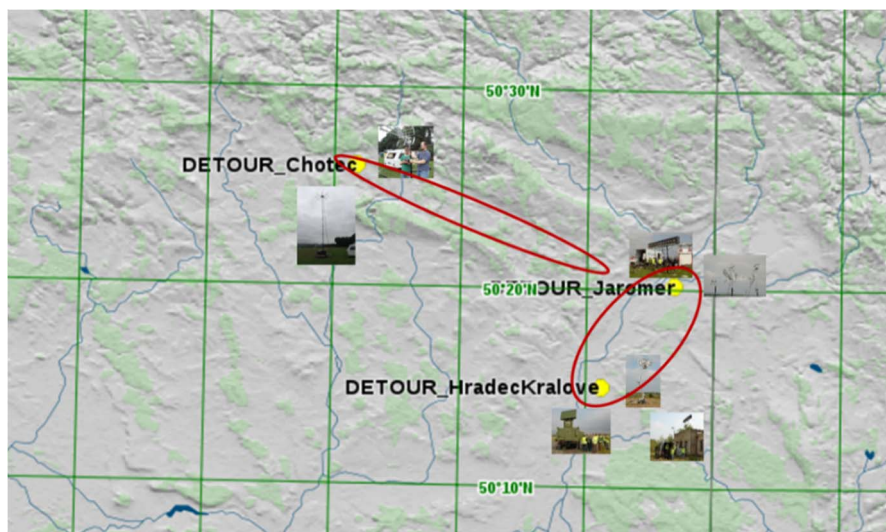


Figure 1 Relief map of the Hradec Kralove district together with the DETOUR sites and systems.

As shown in figure 1, the sensor distribution was intentionally situated in three locations for two reasons: to reach a natural target masking effect by a valley spread out between Chotec and Jaromer, and to take advantage of a wide flat area between Jaromer and Hradec Kralove. Also, at each site the sensors were distributed in such a way so that Passive Coherent Location (PCL) sensors operated on different bands (FM and DVB-T). In addition, in Hradec Kralove these

sensors were collocated with an active dual band radar. Selected sites hosted the following systems:

1. Hradec Kralove airport

- PIT-RADWAR Poland (V)SHORAD radar working in S and C bands
- FFI Norway with DVB-T based PCL system LORA11
- ERA Czech Republic with FM based PCL system Silent Guard [5-6]]

2. Jaromer airfield

- Fraunhofer FHR Germany with DVB-T based PCL system LORA11
- WUT Poland with DVB-T based PCL demonstrator [7-8]

3. Chotec airfield

- WUT Poland with FM [9-11] and DVB-T [7-8] based PCL systems

Trajectories, named Alfa, Bravo...to Foxtrot, were defined to follow objectives such as a low-level attack scenario with low-level terrain masking and shadowing, maneuvering target detection, maximum range detection, target separation, small Radar Cross Section (RCS) target detection, and detection of targets with low velocities. Pilots of different cooperative air targets used their built-in or handheld GPS equipment for trajectory recording and post-mission analyses.

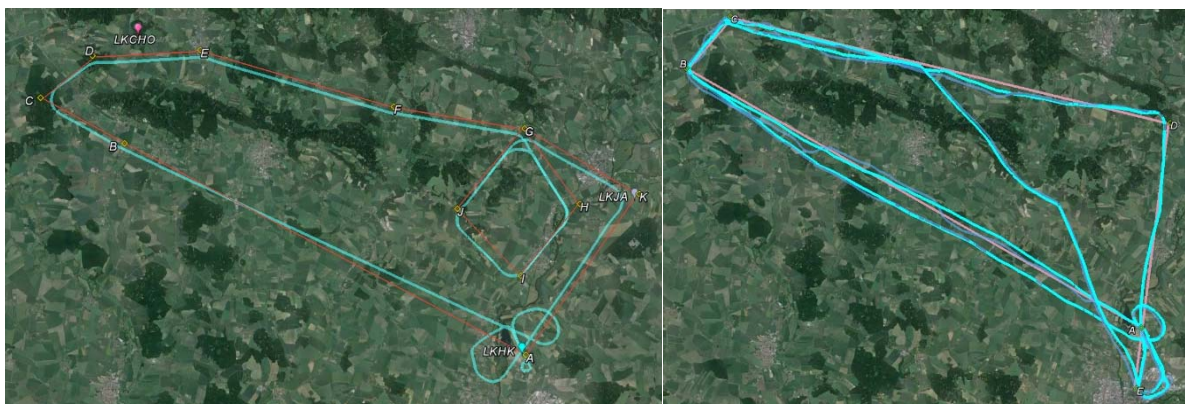


Figure 2 Charlie trajectory with Cessna (red - proposed, blue - flown trajectory) on the left and the Foxtrot trajectory with Delphin and Sting on the right (pink - proposed, light blue - flown by Sting, dark blue - flown by Delphin).

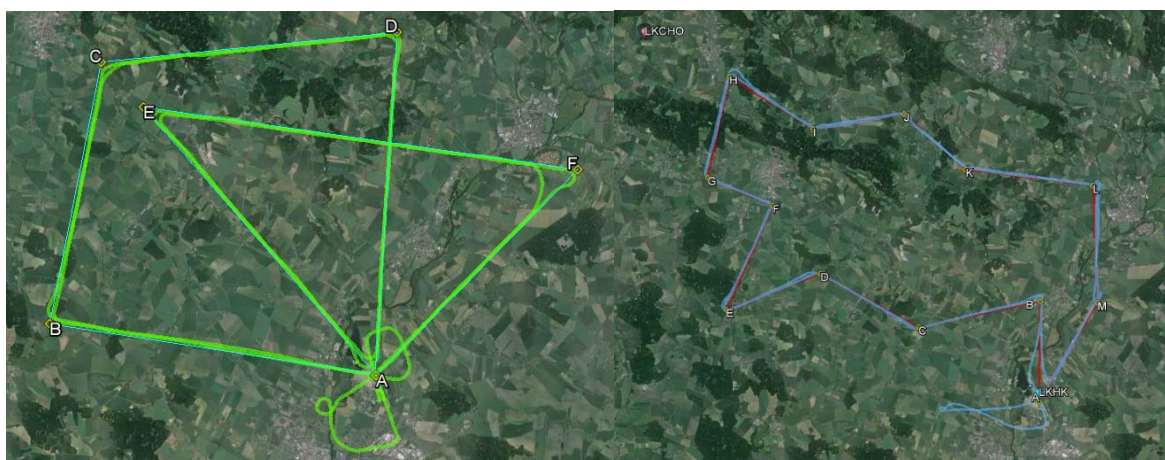


Figure 3 Alpha trajectory with Delphin on the left (blue - proposed trajectory, green - flown trajectory) and Bravo trajectory with a Bell helicopter on the right (red - proposed trajectory, blue - twice flown trajectory).

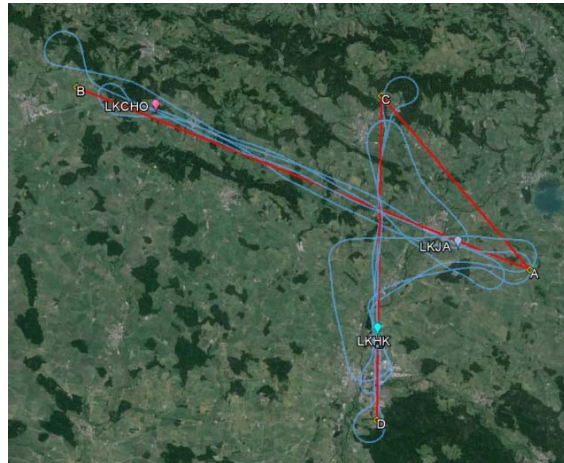


Figure 4 Delta trajectory with a Beechcraft C90 flight (red - proposed trajectory, blue - flown trajectory).



Figure 5 Civil targets: from left Cessna 172, Delphin, Sting TL-2000, Bell 206 and Beechcraft King C90.

### 3. Individual sensor performance

Presentation of all target detection results falls beyond the scope of this paper. Therefore, we introduce one representative measurement sample (for more information see [12]), specifically, of Cessna 172 which in the trials flew following the Charlie trajectory. The Charlie trajectory passed all sensor sites in 3000ft with maneuvers close to two sensor sites (see figure 2). Cessna 172 was selected as an example because it is one of the more popular single engine fixed-wing aircrafts on the one hand and on the other it also represents one kind of potential threats.

A target detection capability is evaluated for the given trajectory in case of the target presence both on the range-Doppler map and in a time-frame as confirmed by an association procedure with a range-Doppler space converted GPS reference. Beside the monostatic/bistatic range and Doppler, a target descriptor contains also standard deviations of the given measurements related to SNR of given detection. The association procedure is as follows.

The first association step is to calculate an association matrix. Each component  $(i, j)$  of the association matrix is a similarity measure which compares the closeness of the  $i$ -th reference data vector  $x_i$  (in fact, we had only one reference data vector,  $x = [distance, velocity]$ ) and the  $j$ -th measurement data vector  $y_j$ . We use the Mahalanobis distance as the measure for association, which is precisely described in [12].

#### WUT FM and DVB-T based PCL demonstrator

An example of one bistatic pair (out of eight applied) detection results with a Praha/Cukrak transmitter of opportunity in a distance of 95km toward the southwest and 38kW power for WUT FM based PCL system placed in the Chotec airfield is shown in figures 6-7.

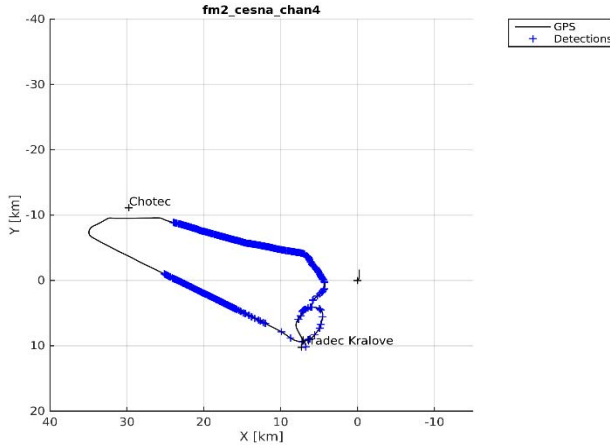


Figure 6 Bistatic detections associated with the GPS reference acquired by C-172 flown following the Charlie trajectory (Praha/Cukrak transmitter of opportunity situated 95km southwest).

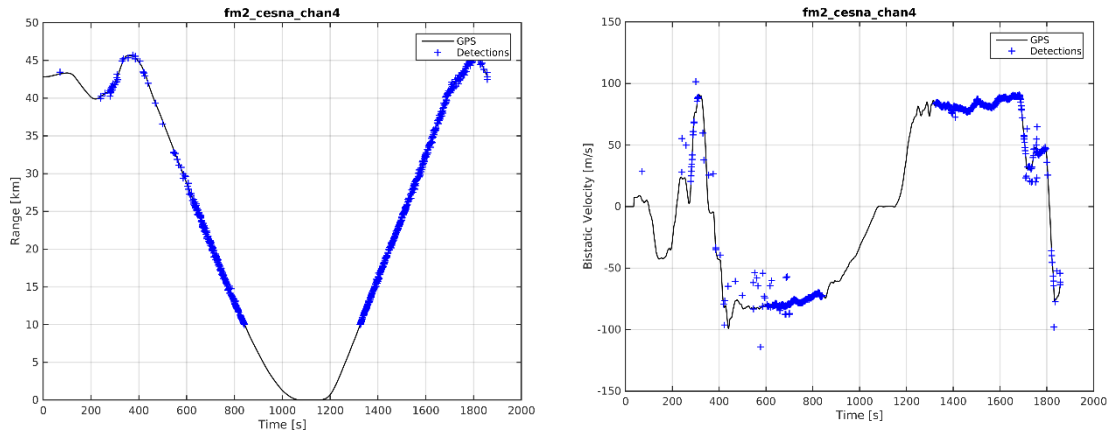


Figure 7 C-172 detection in the bistatic range(left) and the bistatic velocity (right) of C-172.

An example of one bistatic pair (out of four applied) detection results with a Krasne transmitter of opportunity in a distance of 70km toward the south and 100kW power for WUT DVB-T based PCL system placed in the Chotec airfield is shown in figures 8-9.

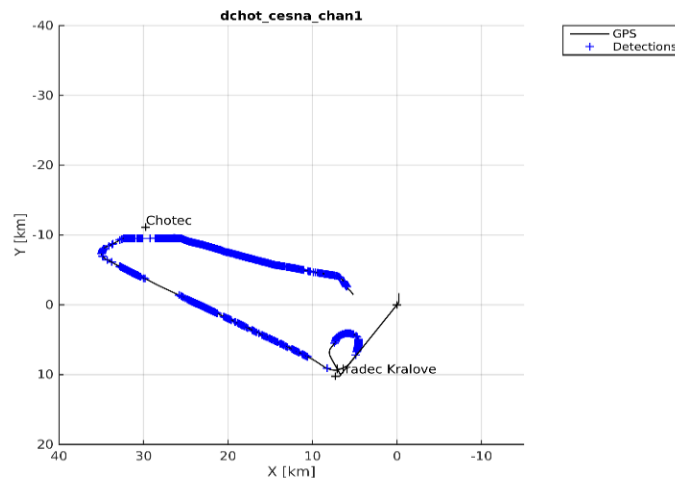


Figure 8 Bistatic detections associated with the GPS reference acquired by C-172 flown following the Charlie trajectory (Krasne transmitter of opportunity situated 70km South).

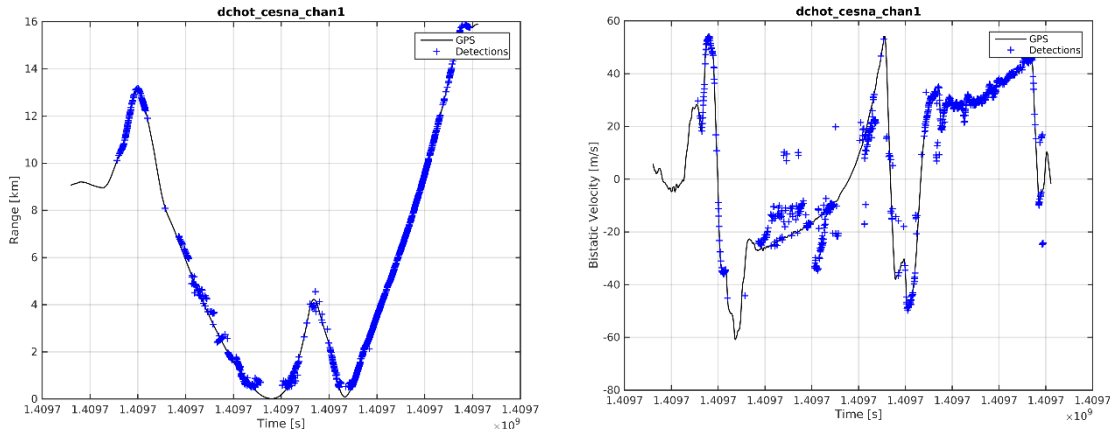


Figure 9 C-172 detection in the bistatic range (left) and the bistatic velocity (right) of C-172.

### FHR DVB-T based PCL demonstrator

The FHR LORA11 11 channel DVB-T PCL system was located in Jaromer using the transmitters at Cerna hora with 100kW power and another one in Krasne, also with 100 kW power. The following figures show the results of a Beechcraft flight No 11b. Figure 10 depicts the detections in the range/Doppler plane and the Cartesian plane, while figure 11 shows the Doppler versus measurement time for the same flight as an example.

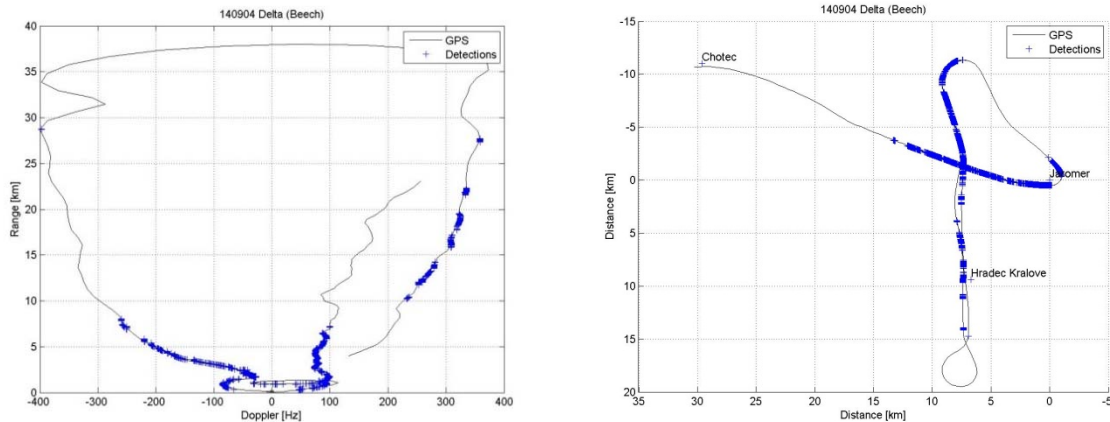


Figure 10 Beechcraft flight 11b detections in range/Doppler (left) and Cartesian plane (right).

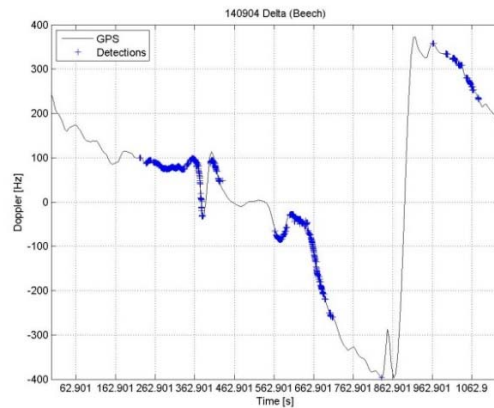


Figure 11 Beechcraft flight 11b Doppler versus measurement times.

### FFI DVB-T based PCL demonstrator

The detection performance of the FFI passive radar is shown in figure 12. The transmitter used was the one at Cerna Hora with 100kW power, situated 45 km north of the sensor. Only a part of the track is visible because of a brief system unavailability during the recording.  $P_{fa}$  was set to  $10^{-3}$ . As it can be seen from the plots, only the area very close to the sensor shows any detection. This can be attributed mostly to the transmitter of opportunity being in the field-of-view of the antenna, as well as being cross-polarized. Higher gain in the analog front-end could have increased the detection rate somewhat.

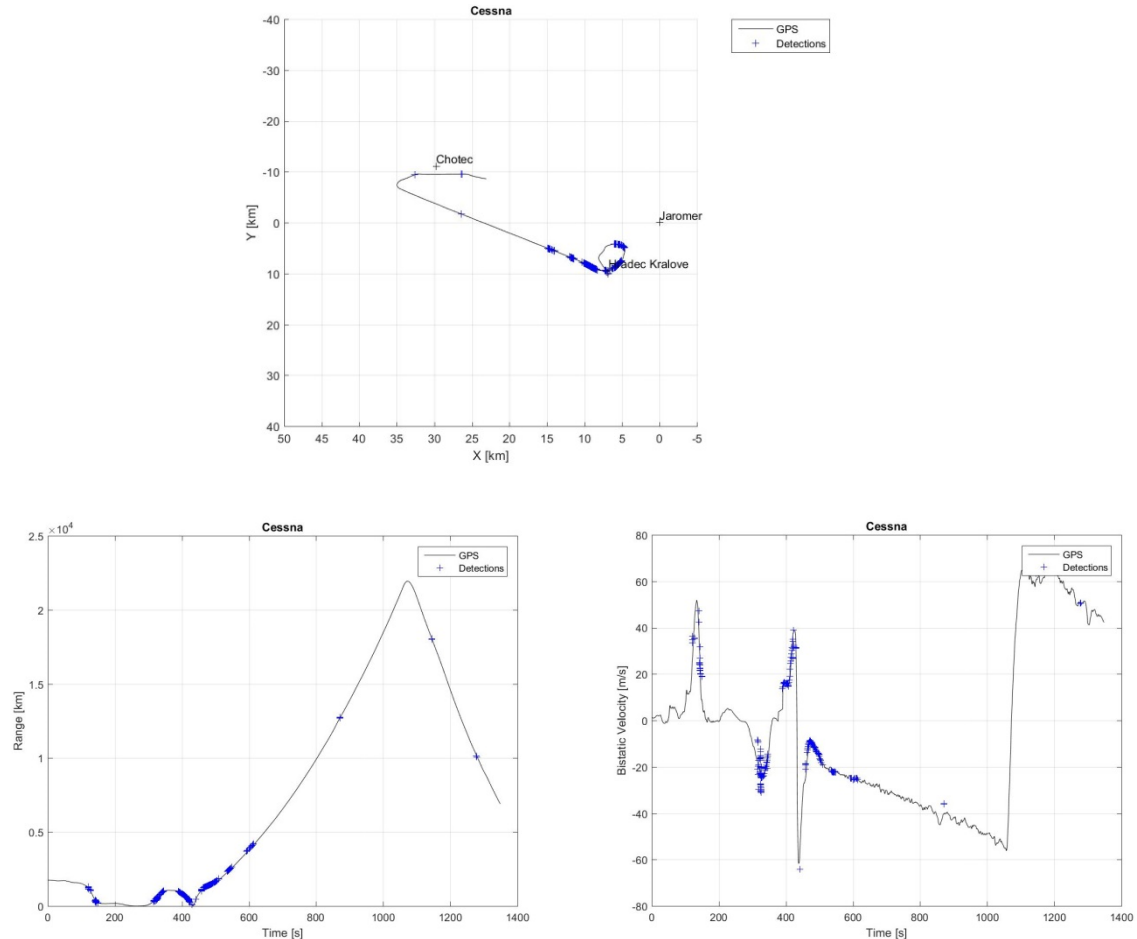


Figure 12 Bistatic detections associated with GPS reference acquired by C-172 flown following the Charlie trajectory (Cerna Hora transmitter of opportunity situated 45km north).  $P_{fa}$  was set to  $10^{-3}$ .

### ERA FM based PCL system

An example of one bistatic pair detection results (out of eight applied) with the Krasne transmitter of opportunity in a distance of 48km toward the south and 100kW power. The presented performance is the best amongst other bistatic pairs due to strong transmitter power, bistatic pair orientation with a surveillance channel direction opposite to Krasne transmitter, and an ideal transmitter coverage.

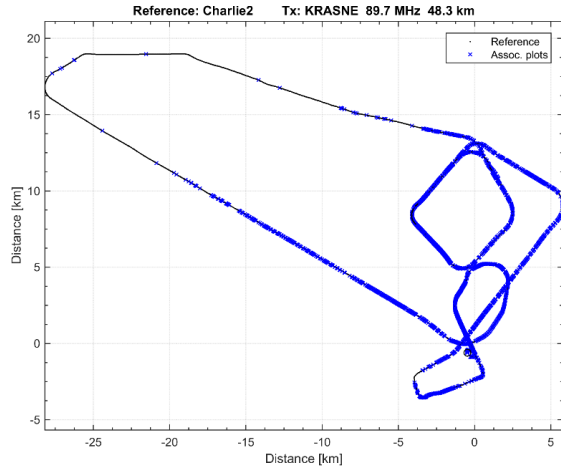


Figure 13 Bistatic detections associated with GPS reference acquired by C-172 flown following the Charlie trajectory (Krasne transmitter of opportunity situated 48km south).

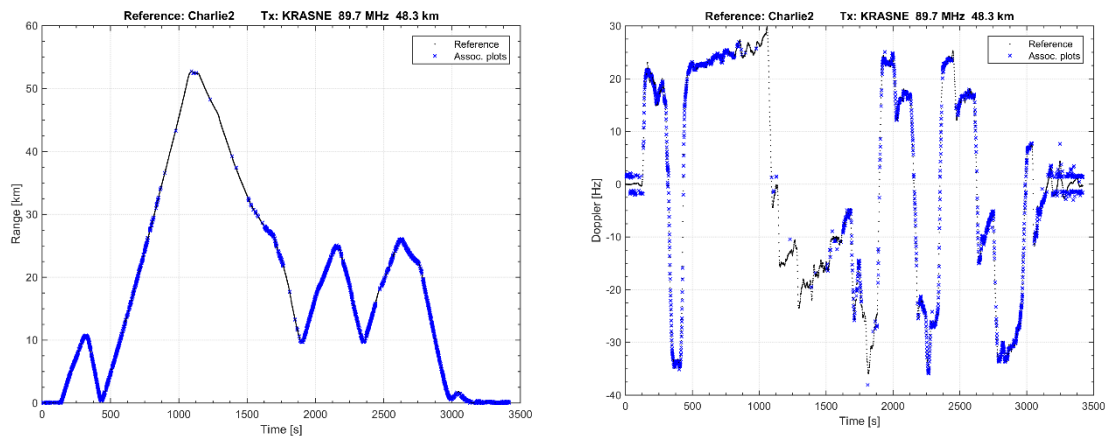


Figure 14 C-172 detection in bistatic range(left) and Doppler (right) of C-172.

#### PIT-RADWAR (V)SHORAD system (the active dual-band radar)

The main idea of signal processing in the dual-band radar demonstrator is presented in chapter 2.1. in [12]. In this section we briefly recall the main processing steps which are performed after an analog-digital conversion.

The signal processing steps are very similar for both the S- and C-band radars with the main difference that following the signal compression, MTD filtering is performed in the case of S-band radar demonstrator while MTI filtering is provided in the case of C-band radar demonstrator. The filtered signals are then processed with the CFAR algorithm. Finally, the incoherent integration of pulses in segments is executed and the resulting values of the signal in each cell are compared with a detection threshold. In order to evaluate the capabilities of the DMPAR system, all values of the processed signals before the plot detection are stored for the chosen tracks.

Examples of the signals recorded in S-band for the selected flight FL2-Charlie are presented below.

Figure 15 shows the raw signal after the signal compression, while figure 16 – the signal completely processed according to the description given above.

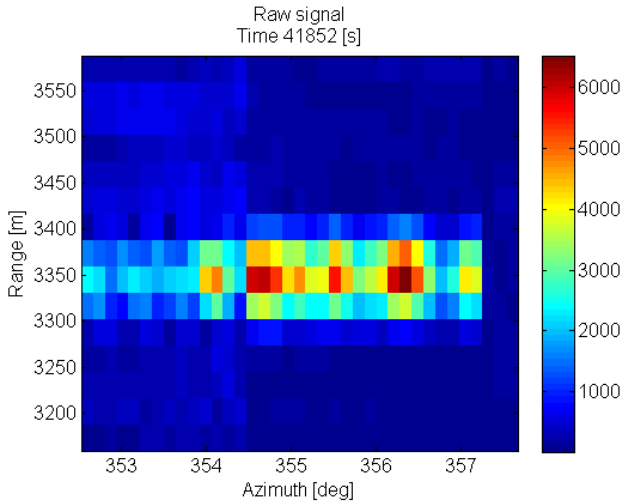


Figure 15 Raw signal after signal compression.

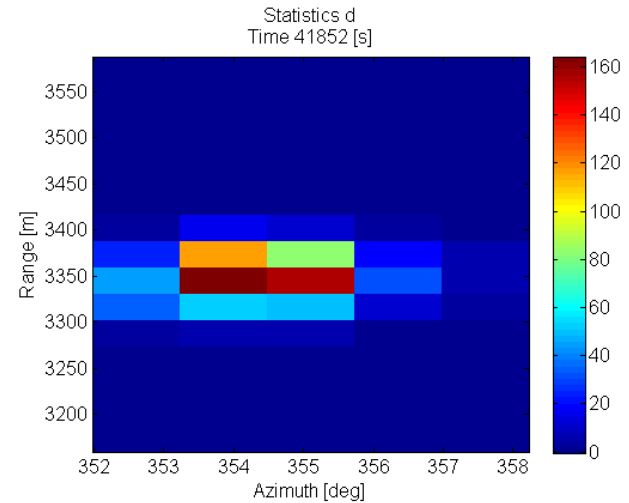


Figure 16 Completely processed signal.

Synchronization with the GPS data, the filtering data and calculation of  $P_{FA}$  are described in detail in [12]. After-processing results for the chosen flight are shown in figure 17.

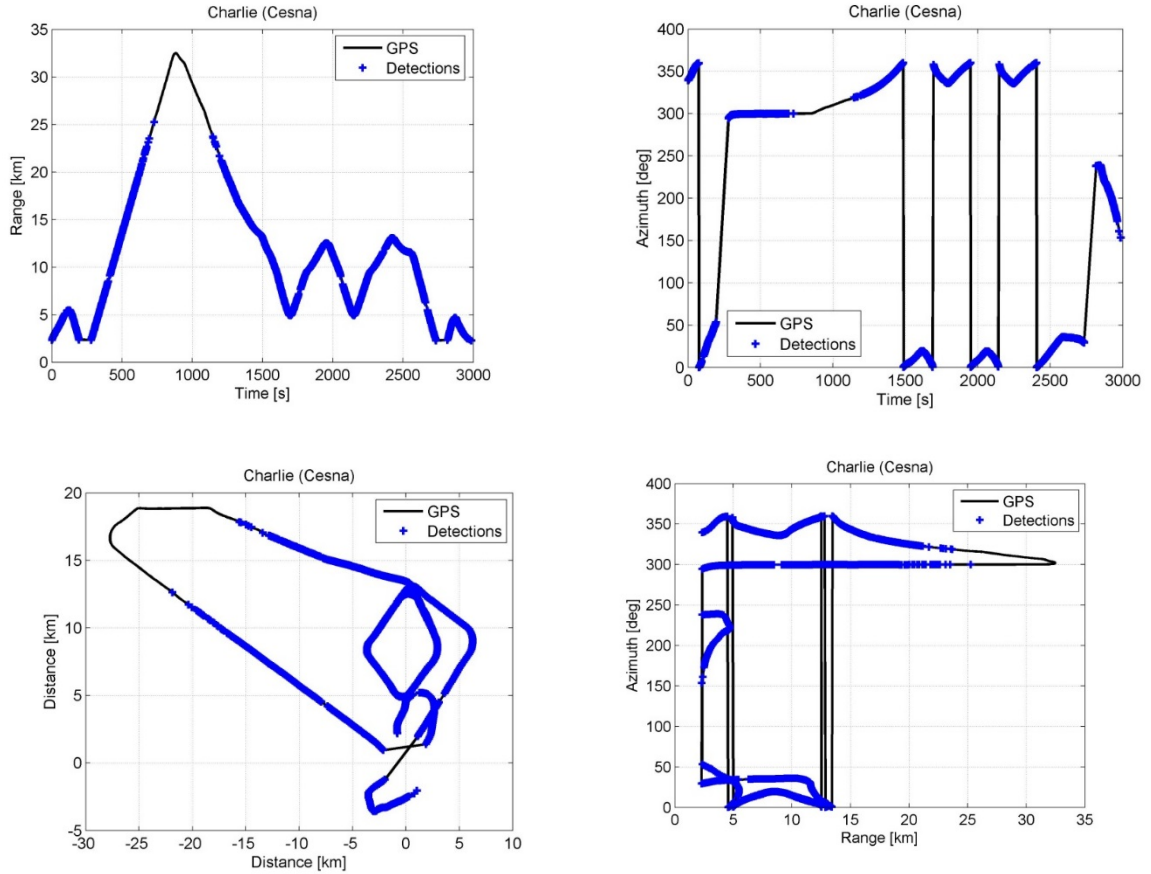


Figure 17 Detections versus sensors for flight 2.

#### 4. DMPAR processing

The DMPAR algorithm developed by PIT-RADWAR used for above mentioned data offline processing is described in [12-13].

The offline processing of the aforementioned algorithms analyzes amplitudes (statistics) of the signals from independent receiving channels of the PCL radar: the DVB-T and FM signals of opportunity. Another sources of the statistics are the receiving channels of the active radar in S- and C-bands. The processing that follows a fusion of these statistics (a signal fusion) is called the centralized detection. Another type of processing applied – called the decentralized detection – is the processing of registered bistatic plots coming separately from passive and active radars (receiving channels are the same as mentioned above).

We assumed that both decentralized and centralized fusions of the DMPAR system consisted of  $N$  individual radars (channels). It means that the channel can be represented by a separate transmitter and/or a separate frequency and/or a separate band.

We set a false track initiation probability to  $10^{-6}$ , resulting in a single refresh integral false alarm probability equal  $4.6 \times 10^{-3}$ . We assumed also that for all channels there was a common refresh period. A structure of the measurement data at the output of each channel (or input of the decentralized or centralized fusion) is in tab. 1.

Tab. 1 The structure of measurement data at output of each channel.

Parameter Name	Description
<b>T</b>	measurement timestamp (aligned to GPS reference from track file)
<b>Lat</b>	latitude position of the object at the given timestamp
<b>Lon</b>	longitude position of the object at the given timestamp
<b>d<sup>2</sup></b>	value of the square amplitude (statistic)
<b>NoiseLevel</b>	noise level estimate
<b>SNR</b>	signal-to-noise ratio for the cell of the statistic
<b>Det</b>	boolean value indicating if SNR exceeds a preselected threshold

The SET-195 main idea was to evaluate the quality improvement based on the DMPAR signal processing. We proposed two statistical rates to evaluate different processing schemes. Based on these rates we made a comparison between the results of the DMPAR processing and, for example, a single sensor processing. These statistical rates were:

- $P_{det}$  – probability of detection as a function of the distance from a specified location,
- $TV$  – track visibility,

The chosen simulation results for flight FL2-Charlie, based on the real collected data, are shown in figure 18 and figure 19.

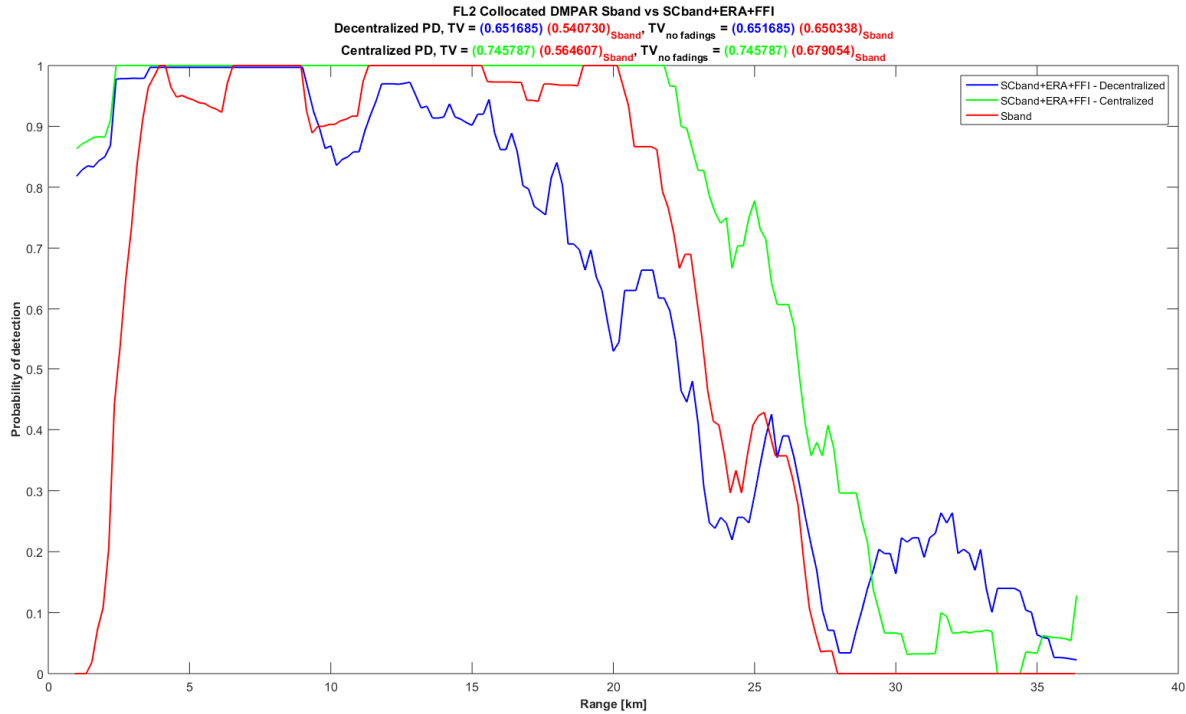


Figure 18 Comparison of detection range in a collocated configuration, flight FL2.

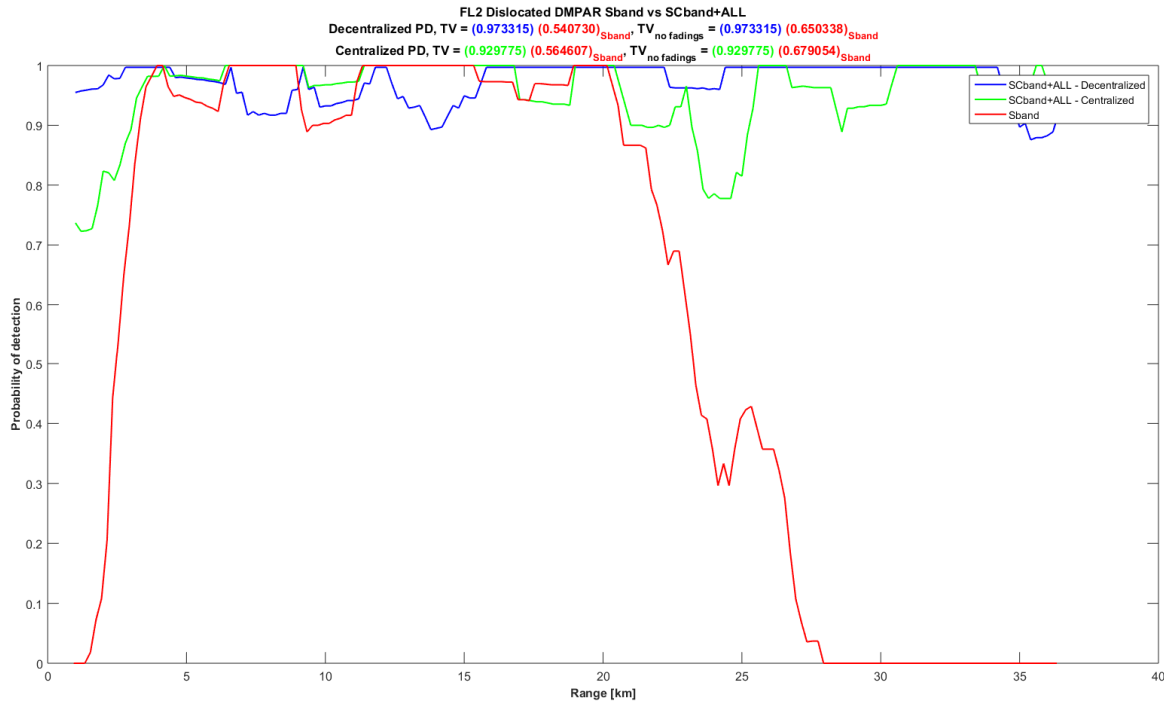


Figure 19 Comparison of detection range in a dislocated configuration, flight FL2.

#### A comparison of the centralized and decentralized processing (Flight FL2 - Charlie)

Figure 18 shows a comparison of the centralized and decentralized processing in case of the collocated antennas (active S- and C-bands, passive FM, passive DVB-T). Please note a lower performance of the decentralized processing in comparison to both centralized one and S-band only processing. This is due to a significant number of sensors with low SNRs (9 passive channels) shadowing relatively small number of sensors with high SNRs (2 active channels). Due to the  $k$  out of  $m$  rule of decentralized detection, the active radar performance is lost because of a number of the passive channels. With the centralized processing, low-SNR channels are scaled down in the threshold statistics, which gives way to the signals from an active component

with a high SNR. In case of far-range detections, most of the channels start to face the low SNR levels and the decentralized processing outperforms the centralized scheme.

Figure 19 shows a comparison of the centralized processing and the decentralized one in case of dislocated antennas (all channels in tab. 2). In contrary to the collocated case, decentralized processing outperforms centralized one in the most part of the range. This may be due to the fact that a far-range region of the active, and passive ERA-FM and FFI-DVB-T components is close-range to the sensors in Jaromer and/or Chotec. Then, at least half of the sensors has the reasonable SNR levels, allowing the decentralized scheme to work, whereas the SNRs remain at the levels too low for the centralized scheme to work (especially, far-range and shadowing for the active component). The coverage in the far-range is mostly provided by the WUT-FM sensor located in Jaromer. In the dislocated case the detection performance is influenced by a trajectory, system configuration and constellation, and a type of the target.

Tab. 2. List of Track Visibility (TV) parameter for all cases in flight FL2.

Scenario	Flight FL2 Analysed case	Decentralized processing		Centralized processing	
		TV	real TV	TV	real TV
Collocated	SCband+ERA+FFI	0,6517	0,6517	0,7458	0,7458
Dislocated	SCband+ALL	0,9733	0,9733	0,9298	0,9298

## 5. Conclusions

During conducted processing of the registered data roughly 130 graphs were generated for different cases, which provided very detailed information for the case presented herein. However, to compare between the centralized and decentralized performances and to have clear results, in this paper we put side by side only the most representative figures and tables concerning the statistical results that can give us general conclusions about the quality of the DMPAR processing.

Considering the need to prove the DMPAR properties, the most important is to compare the results of decentralized and centralized *collocated-sensors* cases. For this purpose, after comparing the curves on figure 18 and figure 19, one can notice that the centralized processing shows definitely better performance. Setting the target probability of detection to 0.9 (a false track initiation probability set to  $10^{-6}$  resulting in the single refresh integral false alarm probability equal  $4.6 \times 10^{-3}$ ), for the FL2 flight one can note a detection range increase in order of 44-47 percent. In the same time TV is about 10% higher for the centralized processing (tab. 2). These results confirm (with data derived from the trials) the trends observed at first during the SET-152 research on simulated data (see figure 20).

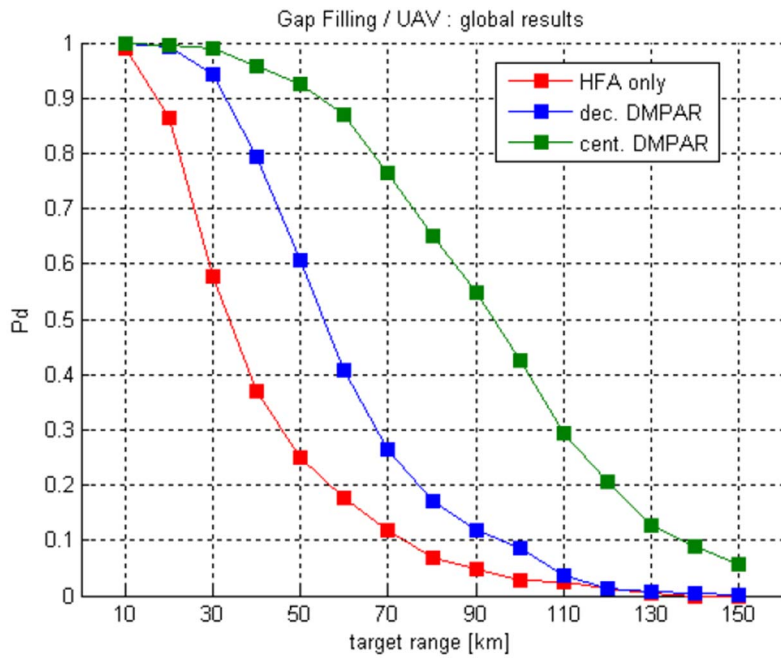


Figure 20 Chosen result from the SET-152 report, shown as a reference for a comparison with the experimental results.

In cases with the dislocated sensors a comparison of the decentralized and centralized processing performances leads to a conclusion that a detection range and TV are dependent on a type of the track, specific terrain settings and the PCL receiver type.

## Acknowledgment

The authors would like to thank the NATO SET CSO for their financial support for the DETOUR trials, and to all individuals from FHR, FFI, ERA, PIT-RADWAR and WUT teams for their hard work in preparation and participation in the trials. In particular, thanks go to the participants from FHR: Jörg Heckenbach, Martin Schroeder, Martin Ummenhofer, Jochen Schell; from FFI: Erlend Finden, Ole Halvard Sætran; from ERA: Pavel Protiva, Martin Vojáček, Veronika Rulcová; from PIT-RADWAR: Lech Raczyński, Leszek Żochowski, Jan Hardejewicz, and from WUT: Mateusz Malanowski, Krzysztof Krawczyk, Marcin Kamil Baczk, Karolina Szczepankiewicz, Michał Szczepankiewicz and Adam Gorzelanczyk.

## References

- [1] Deployable Multi-Band Passive/Active Radar for Air Defense. NATO RTO-TR-SET-152 Technical Report.
- [2] <http://www.era.aero/about-era/press-releases/detour-2014-era-introduced-its-pcl-system-within-nato-exercise>
- [3] V. Stejskal, “PCL and Multilateration System Synergy”, in *Proceedings of International Symposium on Enhanced Solutions for Aircraft and Vehicle Surveillance Applications ESAVE*, Berlin, March 2013.
- [4] V. Stejskal, R. Plšek, M. Pelant, M. Vojáček, “Passive Coherent Location and Passive ESM Tracker Systems Synergy”, in *Proceedings of International Radar Symposium IRS*, Dresden, June 2013.

- [5] [http://www.armyrecognition.com/ide\\_t\\_2013\\_news\\_coverage\\_report\\_pictures\\_video/czech\\_company\\_era\\_launches\\_silent\\_guard\\_mobile\\_demonstrator\\_of\\_passive\\_surveillance\\_system\\_2305133.html](http://www.armyrecognition.com/ide_t_2013_news_coverage_report_pictures_video/czech_company_era_launches_silent_guard_mobile_demonstrator_of_passive_surveillance_system_2305133.html)
- [6] V. Stejskal, R. Plšek, “FM-Based Passive Coherent Location Demonstrator”, in *Proceeding International Symposium: Enhanced Solutions for Aircraft and Vehicle Surveillance Applications*, Berlin, March 2010.
- [7] M. K. Bączyk, P. Krysiak, J. Misiurewicz, P. Samczyński, K. S. Kulpa, *Detection and identification of helicopter rotor using multistatic PCL system based on DVB-T illumination*, in *Proc. of 5th PCL Focus Days 2015*, 28-29 April 2015, Wachtberg, Germany.
- [8] M. K. Bączyk, P. Samczyński, J. Misiurewicz, K. Kulpa, *Micro-Doppler signatures of helicopters in multistatic passive radars*, in IET Radar, Sonar & Navigation, Vol. 9, Issue 9, December 2015, p. 1276 – 1283.
- [9] M. Malanowski, K. Kulpa, M. Mordzonek, P. Samczyński, *PaRaDe – Reconfigurable Software Defined Passive Radar*, RTO NATO SET-136 Specialist Meeting on “Software Defined Radar”, 23-25 June 2009, Lisbon, Portugal.
- [10] M. Malanowski, K. S. Kulpa, J. Kulpa, P. Samczyński, J. Misiurewicz, *Analysis of detection range of FM-based passive radar*, Radar, Sonar & Navigation, IET, vol.8, no.2, February 2014, pp.153,159.
- [11] M. Malanowski, K. Kulpa, P. Samczyński, J. Misiurewicz, J. Kulpa, Ł. Podkalicki, P. Roszkowski, P. Dzwonkowski, D. Gromek, Ł. Maślikowski, M. Misiurewicz, *Experimental results of the PaRaDe passive radar field trials*, in *Proc. on IRS 2012*, 23-25 May 2012, Warszawa, Poland, pp. 65-68.
- [12] DMPAR (Deployable Multi-band Passive/Active Radar for Air Defence) Short-Term Solution Verification. NATO STO SET 195 Technical Report, ISBN 978-92-837-2074-4.
- [13] T. Brenner, L. Lamentowski, L. Raczyński, L. Żochowski, “Off line DMPAR registered signal processing and analysis of the results”, in *STO SM SET 231*, October 2016, Lisbon, Portugal.